



## High-resolution melting analysis to discriminate between the SARS-CoV-2 Omicron variants BA.1 and BA.2

Takuro Koshikawa, Hiroshi Miyoshi\*

Department of Microbiology, St. Marianna University School of Medicine, 2-16-1 Sugao, Miyamae, Kawasaki, 216-8511, Japan

### ARTICLE INFO

#### Keywords:

SARS-CoV-2

Omicron

RBD

HRM analysis

Subvariant

### ABSTRACT

High-resolution melting (HRM) analysis was conducted to discriminate between SARS-CoV-2 Omicron variant BA.1 (B.1.1.529.1) and subvariant BA.2 (B.1.1.529.2). We performed two-step PCR consisting of the first PCR and the second nested PCR to prepare the amplicon for HRM analysis, which detected G339D, N440K, G446S and D796Y variations in the SARS-CoV-2 spike protein. The melting temperatures (Tms) of the amplicons from the cDNA of the Omicron variant BA.1 and subvariant BA.2 receptor binding domain (RBD) in spike protein were the same: 75.2 °C (G339D variation) and 73.4 °C (D796Y variation). These Tms were distinct from those of SARS-CoV-2 isolate Wuhan-Hu-1, and were specific to the Omicron variant. In HRM analyses that detected the N440K and G446S variations, the Tms of amplicons from the cDNA of the Omicron variant BA.1 and subvariant BA.2 RBDs were 73.0 °C (N440K and G446S variations) and 73.5 °C (G446S variation). This difference indicates that the SARS-CoV-2 Omicron variants BA.1 and BA.2 can be clearly discriminated. Our study demonstrates the usefulness of HRM analysis after two-step PCR for the discrimination of SARS-CoV-2 variants.

### 1. Introduction

At the end of 2019, severe acute respiratory syndrome coronavirus 2 (SARS-CoV-2) emerged in China, and caused an outbreak of viral pneumonia. This novel coronavirus disease, also known as coronavirus disease 2019 (COVID-19), has spread rapidly all over the world and has led to a pandemic [1,2]. Mutations in the wild type SARS-CoV-2 (isolate Wuhan-Hu-1) genome have occurred frequently and have increased rapidly, such as those resulting in Lineage B.1.1.7 (Alpha variant), Lineage B.1.617.2 (Delta variant), and Lineage B.1.1.529 (Omicron variant). Lineage B.1.1.529.1 (Omicron BA.1 variant) has been categorized as a variant of concern (VOC) by the World Health Organization (WHO) due to its higher transmissibility and infectivity, and Lineage B.1.1.529.2 ('stealth' Omicron BA.2 variant), a subvariant of the Omicron variant, has recently been detected worldwide. The WHO requested that countries continue to be vigilant, to monitor and report sequences, and to conduct independent and comparative analyses of the different Omicron sublineages [3].

Post-PCR high-resolution melting (HRM) analysis is a highly sensitive molecular biology method based on the melting temperature (Tm)

of amplified double-stranded DNA [4]. Several HRM analyses were previously performed to identify mutations in the SARS-CoV-2 spike protein gene, including in the receptor binding domain (RBD) in spike protein [5–9]. These reports showed that HRM analysis can distinguish between the Tms of the PCR products obtained from the SARS-CoV-2 genome. Furthermore, we previously detected Omicron BA.1-specific G339D (nucleotide mutation: G1016A) and D796Y (nucleotide mutation: G2368T) variations in the SARS-CoV-2 spike protein by post-PCR HRM analysis [10].

The Omicron BA.1 variant has been replaced by the 'stealth' Omicron BA.2 subvariant (B.1.1.529.2) worldwide [3]. The Omicron BA.2 subvariant as well as the Omicron BA.1 variant possesses many mutations in the spike protein gene related to infectivity and vaccination breakthrough cases [11]. Recently, Aoki et al. reported a pilot study to discriminate SARS-CoV-2 BA.1 and BA.2 variants using a high-resolution melting analysis by pre-print [12]. They focused on Omicron BA.1-specific G446S and S477N/T478K and Omicron BA.2-specific R408S variations and S477N/T478K variations. But, their derivative HRM curves had slightly shoulder shape affecting an acquired Tm in those melting peak plots [12]. Therefore, we focused on the

*Abbreviations:* severe acute respiratory syndrome coronavirus 2, SARS-CoV-2; high-resolution melting, HRM; melting temperature, Tm; receptor binding domain, RBD; nucleotide, nt; wild type, wt.

\* Corresponding author.

E-mail address: [hmiyoshi@marianna-u.ac.jp](mailto:hmiyoshi@marianna-u.ac.jp) (H. Miyoshi).

<https://doi.org/10.1016/j.bbrep.2022.101306>

Received 5 June 2022; Received in revised form 23 June 2022; Accepted 28 June 2022

Available online 1 July 2022

2405-5808/© 2022 The Authors. Published by Elsevier B.V. This is an open access article under the CC BY-NC-ND license (<http://creativecommons.org/licenses/by-nc-nd/4.0/>).

Omicron BA.1- and BA.2-specific N440K variation (nucleotide mutation: T1320G) and the Omicron BA.1-specific G446S variation (nucleotide mutation: G1336A) to distinguish the BA.2 subvariant from the Omicron BA.1 variant. In this study, the combination of PCR and post-nested PCR HRM analysis was carried out to discriminate these two variations by using primer sets in our previous study [10]. In this study, the combination of PCR and post-nested PCR HRM analysis was used to discriminate these two variations.

Here, we report an effective and sensitive method for distinguishing between the Omicron BA.1 variant and the BA.2 subvariant. This method is more efficient in detecting mutations than the time-consuming sequencing-based detection method. This report also provides a rapid experimental protocol that can detect new SARS-CoV-2 variants, including the 'Omicron recombinant variant' XE.

## 2. Materials and methods

### 2.1. cDNA synthesis of wt SARS-CoV-2 RBD and SARS-CoV-2 RBD variants

The wild-type SARS-CoV-2 (Isolate Wuhan-Hu-1) RNA genome was purchased from VIRCELL S.L. Complementary DNA fragment synthesis of the RBD (NCBI NC\_045512.2 nt 22,487–24040: 1554 base) in wt SARS-CoV-2 spike protein was performed as described previously [10].

The RBD sequences of the Delta (B.1.617.2), Omicron BA.1 (B.1.1.529.1) and Omicron BA.2 (B.1.1.529.2) variants were obtained from NCBI (<https://www.ncbi.nlm.nih.gov/sars-cov-2/>). Complementary DNA fragments of these RBDs were prepared by site-directed mutagenesis of the synthesized cDNA of the wt SARS-CoV-2 RBD using the primer overlap extension method [13]. The cDNA fragments (1554 bp) of the RBD variants were purified and their sequences were confirmed by agarose gel electrophoresis, gel extraction and DNA sequencing, as described previously [10].

### 2.2. The first PCR amplification of the cDNA of the SARS-CoV-2 RBD

The first PCR was performed as described previously [10]. Each reaction mixture (25  $\mu$ L) contained 0.25 nM forward and reverse primers (Fig. 1 and Supplementary Table 1), 1  $\mu$ L of the abovementioned RBD cDNA (1  $\mu$ g/mL), and PrimeSTAR HS DNA Polymerase (Takara Bio). The PCR amplification consisted of an initial denaturation for 5 s at 98 °C, followed by 40 cycles of denaturation for 10 s at 98 °C, annealing for 5 s at 57 °C and extension for 20 s at 72 °C. The final extension step was carried out at 72 °C for 5 min. After PCR amplification, the reaction mixture was diluted 100,000-fold with sterilized water and used as a template for the subsequent post-nested PCR HRM analysis.

### 2.3. The second amplification step by nested real-time PCR

MeltDoctor HRM Master Mix (Thermo Fisher Scientific) was employed for nested real-time PCR and the subsequent HRM analysis according to the manufacturer's instructions. Primer pairs are shown in Fig. 1 and Supplementary Table 1. The primer pairs were designed to detect Omicron BA.1 and BA.2 variant-specific G339D (nucleotide mutation: G1016A), N440K (nucleotide mutation: T1320G), D796Y (nucleotide mutation: G2368T) and Omicron BA.2 variant-specific G446S (nucleotide mutation: G1336A) variations. Each reaction mixture (20  $\mu$ L) contained 1  $\mu$ L of the first step PCR 100,000-fold dilution mixture, 300 nmol/L of each primer, and 1  $\times$  MeltDoctor HRM Master Mix. The nested real-time PCR and the subsequent HRM analyses were conducted on a QuantStudio 5 real-time PCR system (Thermo Fisher Scientific). The nested PCR amplification was performed under the following conditions: 10 min at 95 °C; 40 cycles of 10 s at 95 °C and 30 s at 60 °C. The fluorescence of the reporter dye was monitored for an extension step at 60 °C.

### 2.4. Post-nested PCR HRM analysis

After amplification by nested real-time PCR, HRM analysis of the amplicon was carried out with denaturation at 95 °C for 10 s, cooling at 60 °C for 60 s and melting curve generation from 60 °C to 95 °C in 0.025 °C/s increments. HRM curves were prepared, and T<sub>m</sub> values were calculated based on the derivative HRM curves by High Resolution Melt Software v.3.2 (Applied Biosystem). The sequences of all amplicons were confirmed by DNA sequencing after HRM analysis.

## 3. Results

### 3.1. Amplification by nested real-time PCR for the wt SARS-CoV-2 RBD and SARS-CoV-2 RBD variants

In the second nested real-time PCR step, amplification was confirmed by the fluorescence signal of reporter dye, as shown in Supplementary Fig. 1. All amplification plots showed similar profiles in which the values of delta R<sub>n</sub> were saturated at  $1.0 \times 10^6$ .

### 3.2. HRM analysis of the amplicon by nested real-time PCR for wt SARS-CoV-2 RBD and SARS-CoV-2 RBD variants

Post-nested PCR HRM analyses of the wt SARS-CoV-2 RBD and SARS-CoV-2 RBD variants were performed in triplicate. Figs. 2 and 3 show representative normalized HRM curves and derivative HRM curves for amplicons of the second step nested PCR respectively.

The normalized HRM curves for amplicons of the Omicron BA.1 variant and BA.2 subvariant exhibited significant differences from the other curves (wt and Delta variant) in the G1016A and G2368T mutation analysis (Fig. 2A and C). The HRM curve for the amplicon of Omicron BA.1 had a similar profile to that of wt SARS-CoV-2 Wuhan-Hu-1 in the detection of the mutations T1320G and G1336A. In contrast, the normalized HRM curve for the amplicon of Omicron BA.2 showed a profile similar to that of the Delta variant (Fig. 2B).

### 3.3. T<sub>m</sub> analyses after nested real-time PCR for wt SARS-CoV-2 RBD and SARS-CoV-2 variant RBDs

T<sub>m</sub>s were acquired by the derivative HRM curves (Fig. 3), as shown in Table 1. The T<sub>m</sub>s of the amplicon obtained from the Omicron BA.1 variant were 75.2 and 73.4 °C, the same as those from the Omicron BA.2 variant, in HRM analyses designed to identify the G339D and D796Y variations (G1016A and G2368T mutations), as shown in Table 1. The T<sub>m</sub>s of these two Omicron variants were distinct from those (75.6–75.7 and 73.9 °C) of wt SARS-CoV-2 Wuhan-Hu-1 and the Delta variant.

In HRM analyses designed to target the N440K and G446S variations (T1320G and G1336A mutations), the T<sub>m</sub> (73.0 °C) obtained from the Omicron BA.1 variant was close to that (72.9 °C) of wt SARS-CoV-2 Wuhan-Hu-1, while the T<sub>m</sub> (73.5 °C) of the Omicron BA.2 variant was close to that (73.4 °C) of the Delta variant (Fig. 3B and Table 1).

## 4. Discussion

We used the same primer pair (Supplementary Table 1) as our previous report [10] to confirm the efficacy of a second nested PCR for the detection of all mutations (G1016A, T1320G, G1336A and G2368T) in this study. All R<sub>n</sub> values of the amplification plot obtained in the second nested real-time PCR were saturated at  $1.0 \times 10^6$  (Supplementary Fig. 1). This saturation of R<sub>n</sub> values and the profiles of the amplification plots clearly show that the amplicons from the nested PCR were derived from SARS-CoV-2 genes. We then analysed the amplified products obtained from the first PCR and the second nested real-time PCR by agarose gel electrophoresis. All amplicons from the second nested real-time PCR appeared as a single band on the agarose gel (Supplementary Fig. 2, e.g., target G1016A mutation). This convergence to a

<b>A</b>		925	956
Isolate Wuhan-Hu-1		gaaaaaggaatctatcaaacttctaacttttagagtccaaccaacagaatctattggttaga	
Delta variant		gaaaaaggaatctatcaaacttctaacttttagagtccaaccaacagaatctattggttaga	
Omicron BA.1 variant		gaaaaaggaatctatcaaacttctaacttttagagtccaaccaacagaatctattggttaga	
BA.2 subvariant		gaaaaaggaatctatcaaacttctaacttttagagtccaaccaacagaatctattggttaga	
			1016
Isolate Wuhan-Hu-1		tttcctaataattacaaacttgtgccccttttggatgaagtttttaacgccaccagatttgca	
Delta variant		tttcctaataattacaaacttgtgccccttttggatgaagtttttaacgccaccagatttgca	
Omicron BA.1 variant		tttcctaataattacaaacttgtgccccttttggatgaagtttttaacgccaccagatttgca	
BA.2 subvariant		tttcctaataattacaaacttgtgccccttttggatgaagtttttaacgccaccagatttgca	
		1048	1078
Isolate Wuhan-Hu-1		tctgtttatgcttggaaacaggaagagaatcagcaactgtgttgctgattattctgtccta	
Delta variant		tctgtttatgcttggaaacaggaagagaatcagcaactgtgttgctgattattctgtccta	
Omicron BA.1 variant		tctgtttatgcttggaaacaggaagagaatcagcaactgtgttgctgattattctgtccta	
BA.2 subvariant		tctgtttatgcttggaaacaggaagagaatcagcaactgtgttgctgattattctgtccta	
<b>B</b>		1225	1239
Isolate Wuhan-Hu-1		caaatcgctccagggcaaaactggaagattgctgattataaattataaattaccagatgat	
Delta variant		caaatcgctccagggcaaaactggaagattgctgattataaattataaattaccagatgat	
Omicron BA.1 variant		caaatcgctccagggcaaaactggaagattgctgattataaattataaattaccagatgat	
BA.2 subvariant		caaatcgctccagggcaaaactggaagattgctgattataaattataaattaccagatgat	
		1290	1320
Isolate Wuhan-Hu-1		tttacaggctgctttagcttggaaattctaacaactcttgattctaagggttggtggtaat	
Delta variant		tttacaggctgctttagcttggaaattctaacaactcttgattctaagggttggtggtaat	
Omicron BA.1 variant		tttacaggctgctttagcttggaaattctaacaactcttgattctaagggttggtggtaat	
BA.2 subvariant		tttacaggctgctttagcttggaaattctaacaactcttgattctaagggttggtggtaat	
		1335	1370
Isolate Wuhan-Hu-1		tataattacctgtatagattgtttaggaagtctaactctcaaaccttttgagagagatatt	
Delta variant		tataattacctgtatagattgtttaggaagtctaactctcaaaccttttgagagagatatt	
Omicron BA.1 variant		tataattacctgtatagattgtttaggaagtctaactctcaaaccttttgagagagatatt	
BA.2 subvariant		tataattacctgtatagattgtttaggaagtctaactctcaaaccttttgagagagatatt	
		1417	
Isolate Wuhan-Hu-1		tcaactgaaatctatcagggccggtagcacacaccttgtaatgggtgttgaaggttttaattgt	
Delta variant		tcaactgaaatctatcagggccggtagcacacaccttgtaatgggtgttgaaggttttaattgt	
Omicron BA.1 variant		tcaactgaaatctatcagggccggtagcacacaccttgtaatgggtgttgaaggttttaattgt	
BA.2 subvariant		tcaactgaaatctatcagggccggtagcacacaccttgtaatgggtgttgaaggttttaattgt	
<b>C</b>		2307	2334
Isolate Wuhan-Hu-1		ggaatagctggttgaacaagacaaaaacccaagaagtttttgcacaagtcaaacaaatt	
Delta variant		ggaatagctggttgaacaagacaaaaacccaagaagtttttgcacaagtcaaacaaatt	
Omicron BA.1 variant		ggaatagctggttgaacaagacaaaaacccaagaagtttttgcacaagtcaaacaaatt	
BA.2 subvariant		ggaatagctggttgaacaagacaaaaacccaagaagtttttgcacaagtcaaacaaatt	
			2368
Isolate Wuhan-Hu-1		tacaaaaaccaccaattaaagattttgggtggttttaatttttcacaaatattaccagat	
Delta variant		tacaaaaaccaccaattaaagattttgggtggttttaatttttcacaaatattaccagat	
Omicron BA.1 variant		tacaaaaaccaccaattaaatattttgggtggttttaatttttcacaaatattaccagat	
BA.2 subvariant		tacaaaaaccaccaattaaatattttgggtggttttaatttttcacaaatattaccagat	
		2428	2445
Isolate Wuhan-Hu-1		ccatcaaaaaccaagcaagaggtcatttattgaagatctacttttcaacaaagt	
Delta variant		ccatcaaaaaccaagcaagaggtcatttattgaagatctacttttcaacaaagt	
Omicron BA.1 variant		ccatcaaaaaccaagcaagaggtcatttattgaagatctacttttcaacaaagt	
BA.2 subvariant		ccatcaaaaaccaagcaagaggtcatttattgaagatctacttttcaacaaagt	

**Fig. 1.** Comparisons of the SARS-CoV-2 Wuhan-Hu-1 isolate, Delta variant, Omicron variant BA.1 and Omicron subvariant BA.2 sequences.

(A) Sequence position at SARS-CoV-2 Isolate Wuhan-Hu-1: nt925 – nt1104. (B) Sequence position at SARS-CoV-2 Isolate Wuhan-Hu-1: nt1225 – nt1464. (C) Sequence position at SARS-CoV-2 Isolate Wuhan-Hu-1: nt2307 – nt2478. Nucleotide numbers are positioned at spike protein gene in SARS-CoV-2 isolate Wuhan-Hu-1 genome (NC\_045512.2).

Shading indicates the sequence of the primer used for amplification in the first PCR step, and plain and italic letters indicate the sequences of the forward and reverse primers, respectively. The underline indicates the sequence of the primer for the second nested real-time PCR, and plain and italic letters indicate the sequences of the forward and reverse primers, respectively. The targeted mutations in the HRM analysis are shown in capital letters. All amplicons from the second nested real-time PCR step were obtained from the product of the first PCR amplification against cDNA (nt 925–2478) of *wt* SARS-CoV-2 RBD and SARS-CoV-2 RBD variants. Amplicons obtained from the second amplification by nested real-time PCR were 115 bp (nt956 – nt1070), 105 bp (nt1290 – nt1394) and 115 bp (nt2334 – nt2448).

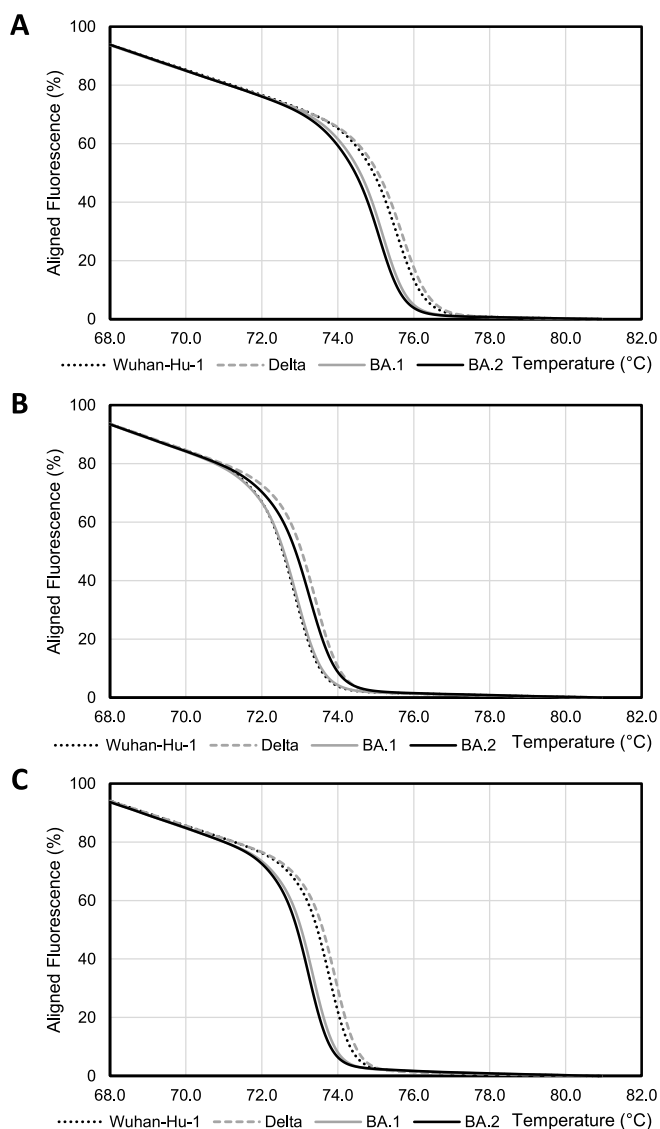


**Fig. 2.** Normalized HRM curves for amplicons of the SARS-CoV-2 Wuhan-Hu-1 isolate RBD and SARS-CoV-2 variant RBDs.

(A) Normalized HRM curves of amplicons from the second nested PCR amplification with the primer pair “Second G339D forward” and “Second G339D reverse” to detect the G1016A mutation.

(B) Normalized HRM curves of amplicons from the second nested PCR amplification with the primer pair “Second N440K and G446S forward” and “Second N440K and G446S reverse” to detect the T1320G and G1336A mutations.

(C) Normalized HRM curves of amplicons from the second nested PCR amplification with the primer pair “Second D796Y forward” and “Second D796Y reverse” to detect the G2368T mutation.

Black dotted lines indicate HRM curves for amplicons from the cDNA of SARS-CoV-2 Wuhan-Hu-1 isolate RBD. Grey broken lines indicate HRM curves for amplicons from the cDNA of SARS-CoV-2 Delta variant RBD. Grey solid lines indicate HRM curves for amplicons from the cDNA of SARS-CoV-2 Omicron BA.1 variant RBD. Black solid lines indicate HRM curves for amplicons of SARS-CoV-2 Omicron BA.2 subvariant RBD. HRM analyses were performed three times, the mean  $T_m$  was calculated. A representative curve is shown in this figure.

single band demonstrated the efficacy of the second nested PCR and corresponds with the Rn saturation on the amplification plot. In addition, the HRM curves for the detection of the mutation T1335G showed significant differences between Delta variant and *wt* SARS-CoV-2 Wuhan-Hu-1 (Figs. 2B and 3B.). These differences were consistent

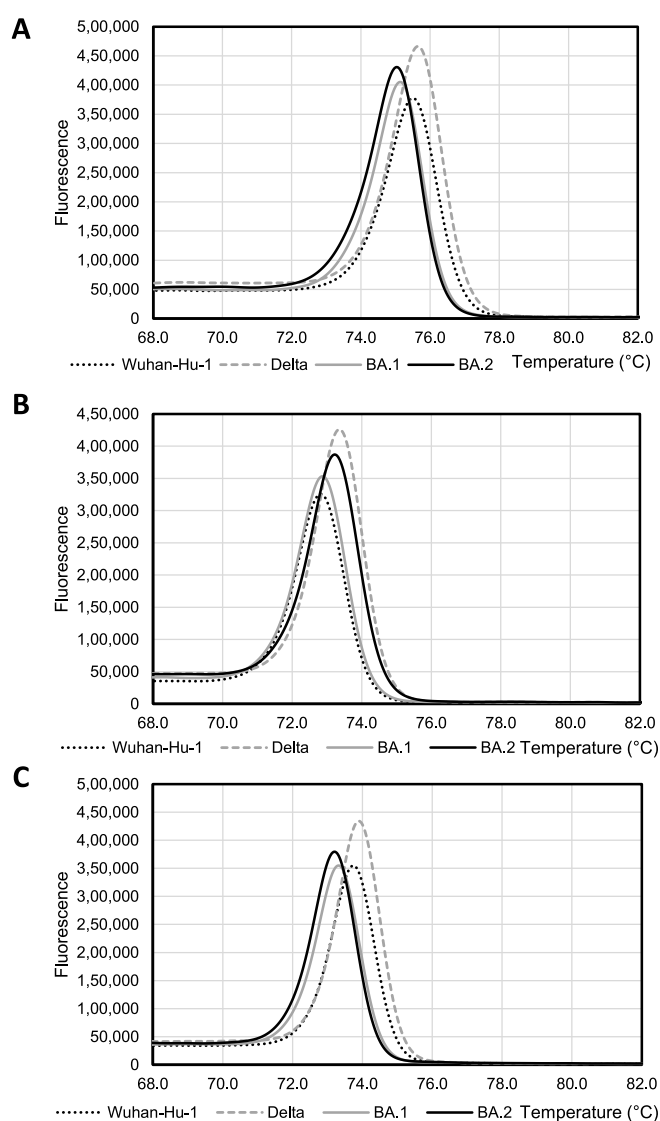


**Fig. 3.** Derivative HRM curves for amplicons of SARS-CoV-2 Wuhan-Hu-1 isolate RBD and SARS-CoV-2 variant RBDs.

(A) Derivative HRM curves of amplicons from the second nested PCR amplification with the primer pair “Second G339D forward” and “Second G339D reverse” to detect the G1016A mutation.

(B) Derivative HRM curves of amplicons from the second nested PCR amplification with the primer pair “Second N440K and G446S forward” and “Second N440K and G446S reverse” to detect the T1320G and G1336A mutations.

(C) Derivative HRM curves of amplicons from the second nested PCR amplification with the primer pair “Second D796Y forward” and “Second D796Y reverse” to detect the G2368T mutation.

Black dotted lines indicate HRM curves for amplicons of the SARS-CoV-2 Wuhan-Hu-1 isolate RBD. Grey broken lines indicate HRM curves for amplicons of SARS-CoV-2 Delta variant RBD. Grey solid lines indicate HRM curves for amplicons of the SARS-CoV-2 Omicron BA.1 variant RBD. Black solid lines indicate HRM curves for amplicons of the SARS-CoV-2 Omicron BA.2 subvariant RBD. HRM analyses were performed three times, the mean  $T_m$  was calculated. A representative curve is shown in this figure.

with the results reported by Aoki et al. and our group [10,14]. Collectively, these results demonstrate the efficacy of the post-nested PCR HRM analysis in this study.

The HRM curves of Omicron BA.2 variants did not show significant differences from those of the Omicron BA.1 variant in the detection of the G339D (mutation G1016A) and D796Y (mutation G2368T)

**Table 1**

Tms of nested PCR amplicons of the SARS-CoV-2 RBD isolate Wuhan-Hu-1 and SARS-CoV-2 RBD variants.

Target variation (Nucleotide mutation)	Mean Tm of the Wuhan-Hu-1 RBD (°C)	Mean Tm of the Delta variant RBD (°C)	Mean Tm of the Omicron BA.1 variant RBD (°C)	Mean Tm of the Omicron BA.2 variant RBD (°C)
G339D (G1016A)	75.6	75.7	75.2	75.2
N440K, G446S (T1320G, G1336A)	72.9	73.4	73.0	73.5
D796Y (G2368T)	73.9	73.9	73.4	73.4

Tms were calculated from the derivative HRM curves (Fig. 3A, B and C). HRM analyses were performed three times, the mean Tm was calculated.

variations (Fig. 2A and C). As shown in Table 1, the Tms of the amplicons from the Omicron BA.1 and BA.2 variants were 75.2 and 73.4 °C. These Tms were lower than those of *wt* SARS-CoV-2 Wuhan-Hu-1 and the Delta variant (75.6–75.7 and 73.9 °C), as shown in Table 1. Therefore, a decrease in the Tm of the amplicon in the detection of the G1016A and G2368T mutations compared to the Tm of *wt* SARS-CoV-2 Wuhan-Hu-1 means that the amplicon derives from the Omicron BA.1 or BA.2 variant.

In the detection of the N440K and G446S variations (mutations T1320G and G1336A), the HRM curve of the amplicon of the Omicron BA.2 variant was considerably different from that of the Omicron BA.1 variant (Fig. 2B). As shown in Table 1, The Tms obtained from the amplicons of the Omicron BA.1 and BA.2 variants were 73.0 and 73.5 °C. In contrast, there were no significant differences between the Tm (73.0 °C) of the amplicon from Omicron BA.1 and that (72.9 °C) of *wt* SARS-CoV-2 Wuhan-Hu-1 because the positive effect of the T1320G mutation on the Tm of the amplicon counteracted the negative effect of the G1336A mutation on the Tm of the amplicon, as reported previously [10]. Since the amplicons from the Omicron BA.2 and Delta variants are the same length (105 bp) and the same kind of mutation (T1335G and T1320G) was present in their amplicon (Fig. 1 and Supplementary Table 1), the Tm (73.5 °C) of the amplicon of Omicron BA.2 was close to that (73.4 °C) of the Delta variant. Taken together, these results indicate that HRM analysis for the detection of the N440K and G446S variations (mutations T1320G and G2368A) can be used to distinguish between the Omicron BA.1 variant and BA.2 subvariant.

In a previous study, we showed that the HRM curves and Tms obtained from an Omicron variant-positive specimen by using the same primer pairs were consistent with those of the cDNA amplicon of Omicron variant RBD [10]. In this study, the amplicon obtained by nested real-time PCR shows saturated Rn values on the amplification plot (Supplementary Fig. 1), and the saturation of the Rn value means that the amplicon obtained by nested PCR is derived from the SARS-CoV-2 gene. Given this consistency, this study indicates that post-PCR HRM analyses in the detection of G1016A, G1336A, T1320G and G2368T mutations can identify SARS-CoV-2 Omicron variants from SARS-CoV-2-positive specimen and that the HRM analysis can be applied to discriminate between the Omicron BA.1 variant and BA.2 subvariant.

Here, we report the discrimination between the SARS-CoV-2 Omicron BA.1 and BA.2 variants by HRM analysis of nested PCR amplicons. This method can be applied to discriminate various virus variations by designing an adequate oligonucleotide primer, and could be adapted to screen SARS-CoV-2 variants.

## Declaration of competing interest

The authors declare that they have no known competing financial interests or personal relationships that could have appeared to influence the work reported in this paper.

## Appendix A. Supplementary data

Supplementary data to this article can be found online at <https://doi.org/10.1016/j.bbrep.2022.101306>.

## References

- [1] D.S. Hui, E. I. Azhar, T.A. Madani, F. Ntoumi, R. Kock, O. Dar, G. Ippolito, T. D. McHugh, Z.A. Memish, C. Drosten, A. Zumla, E. Petersen, The continuing 2019-nCoV epidemic threat of novel coronaviruses to global health — the latest 2019 novel coronavirus outbreak in Wuhan, China., *Int. J. Infect. Dis.* 91 (2020) 264–266, <https://doi.org/10.1016/j.ijid.2020.01.009>.
- [2] J.T. Wu, K. Leung, G.M. Leung, Nowcasting and forecasting the potential domestic and international spread of the 2019-nCoV outbreak originating in Wuhan, China: a modelling study, *Lancet* 395 (2020) 689–697, [https://doi.org/10.1016/s0140-6736\(20\)30260-9](https://doi.org/10.1016/s0140-6736(20)30260-9).
- [3] World Health Organization, Statement on Omicron sublineage BA. <https://www.who.int/news/item/22-02-2022-statement-on-omicron-sublineage-ba-2>, 2022. (Accessed 9 April 2022), 2.
- [4] G.H. Reed, J.O. Kent, C.T. Wittwer, High-resolution DNA melting analysis for simple and efficient molecular diagnostics, *Pharmacogenomics* 8 (2007) 597–608, <https://doi.org/10.2217/14622416.8.6.597>.
- [5] F.M. Gazali, M. Nuhamunada, R. Nabilla, E. Supriyati, M.S. Hakim, E. Arguni, E. W. Daniwijaya, T. Nuryastuti, S.M. Haryana, T. Wibawa, N. Wijayanti, Detection of SARS-CoV-2 spike protein D614G mutation by qPCR-HRM analysis, *Heliyon* 7 (2021), e07936, <https://doi.org/10.1016/j.heliyon.2021.e07936>.
- [6] B.I.d.S. Ferreira, N.L. da Silva-Gomes, W.L. Coelho, V.D. da Costa, V.C.d. S. Carneiro, R.L. Kader, M.P. Amaro, L.M. Villar, F. Miyajima, S.V. Alves-Leon, V. S. de Paula, L.A.A. Leon, O.C. Moreira, Validation of a novel molecular assay to the diagnostic of COVID-19 based on real time PCR with high resolution melting, *PLoS One* 16 (2021), e0260087, <https://doi.org/10.1371/journal.pone.0260087>.
- [7] H. Diaz-García, A.L. Guzmán-Ortiz, T. Angeles-Floriano, I. Parra-Ortega, B. López-Martínez, M. Martínez-Saucedo, G. Aquino-Jarquín, R. Sánchez-Urbina, H. Quezada, J.T. Granados-Riveron, Genotyping of the major SARS-CoV-2 clade by short-amplicon high-resolution melting (SA-HRM) analysis, *Genes* 12 (2021) 531.
- [8] M.J. Kalita, K. Dutta, G. Hazarika, R. Dutta, S. Kalita, P.P. Das, M.P. Sarma, S. Banu, M.G. Idris, A.J. Talukdar, S. Dutta, A. Sharma, S. Medhi, In-house reverse transcriptase polymerase chain reaction for detection of SARS-CoV-2 with increased sensitivity, *Sci. Rep.* 11 (2021) 17878, <https://doi.org/10.1038/s41598-021-97502-1>.
- [9] A. Aoki, Y. Mori, Y. Okamoto, H. Jinno, Development of a genotyping platform for SARS-CoV-2 variants using high-resolution melting analysis, *J. Infect. Chemother.* 27 (2021) 1336–1341, <https://doi.org/10.1016/j.jiac.2021.06.007>.
- [10] H. Miyoshi, R. Ichinohe, T. Koshikawa, High-resolution melting analysis after nested PCR for the detection of SARS-CoV-2 spike protein G339D and D796Y variations, *Biochem. Biophys. Res. Commun.* 606 (2022) 128–134, <https://doi.org/10.1016/j.bbrc.2022.03.083>.
- [11] J. Fonager, M. Bennedbaek, P. Bager, J. Wohlfahrt, K.M. Ellegaard, A.C. Ingham, S. M. Edslev, M. Stegger, R.N. Sieber, R. Lassauniere, A. Fomsgaard, T. Lillebaek, C. W. Svarrer, F.T. Møller, C.H. Møller, R. Legarth, T.V. Sydenham, K. Steinke, S. J. Paulsen, J.A.S. Castruita, U.V. Schneider, C.H. Schouw, X.C. Nielsen, M. Overvad, R.T. Nielsen, R.L. Marvig, M.S. Pedersen, L. Nielsen, L.L. Nilsson, J. Bybjerg-Grauholm, I.H. Tarpgaard, T.S. Ebsen, J.U.H. Lam, V. Gunalan, M. Rasmussen, Molecular epidemiology of the SARS-CoV-2 variant Omicron BA.2 sub-lineage in Denmark, 29 november 2021 to 2 january 2022, *Euro Surveill.* 27 (2022), 2200181, <https://doi.org/10.2807/1560-7917.es.2022.27.10.2200181>.
- [12] A. Aoki, H. Adachi, Y. Mori, M. Ito, K. Sato, K. Okuda, T. Sakakibara, Y. Okamoto, H. Jinno, Discrimination of SARS-CoV-2 Omicron sub-lineages BA.1 and BA.2 using a high-resolution melting-based assay: a pilot study, *bioRxiv* (2022), <https://doi.org/10.1101/2022.04.11.487970>, 2022.2004.2011.487970.
- [13] R.M. Horton, H.D. Hunt, S.N. Ho, J.K. Pullen, L.R. Pease, Engineering hybrid genes without the use of restriction enzymes: gene splicing by overlap extension, *Gene* 77 (1989) 61–68, [https://doi.org/10.1016/0378-1119\(89\)90359-4](https://doi.org/10.1016/0378-1119(89)90359-4).
- [14] A. Aoki, H. Adachi, Y. Mori, M. Ito, K. Sato, K. Okuda, T. Sakakibara, Y. Okamoto, H. Jinno, A rapid screening assay for L452R and T478K spike mutations in SARS-CoV-2 Delta variant using high-resolution melting analysis, *J. Toxicol. Sci.* 46 (2021) 471–476, <https://doi.org/10.2131/jts.46.471>.